

Bimetallic Intermediates in the Formation of Nucleophilic Allenylzincs from Allenylpalladiums: A DFT Study

Rosana Álvarez* and Angel R. de Lera

Departamento de Química Orgánica, Facultad de Química, Universidade de Vigo, Lagoas-Marcosende s/n, 36310 Vigo, Spain

José M. Aurrecoechea* and Aritz Durana

Departamento de Química Orgánica II, Facultad de Ciencia y Tecnología, Universidad del País Vasco, Apartado 644, 48080 Bilbao, Spain

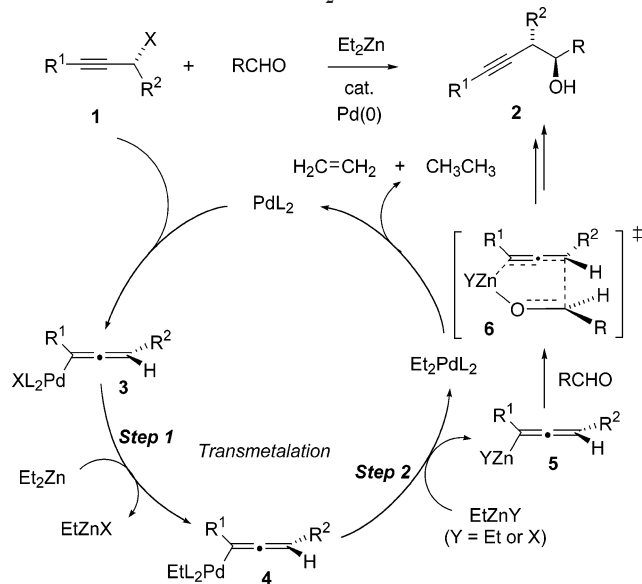
Received December 19, 2006

Summary: According to DFT calculations, allenyl transfer from Pd to Zn may take place through intermediate bimetallic Pd–Zn complexes and be facilitated by the intermetallic link. The resulting bimetallic allenylzinc species display typical nucleophilic behavior in carbonyl addition reactions.

The Pd(0)-catalyzed/Et₂Zn-promoted intermolecular coupling between propargylic mesylates or benzoates **1** (X = OMs, OBz) and aldehydes is a powerful C–C bond-forming reaction that enables the efficient preparation of homopropargyl alcohols **2** (Scheme 1).¹ This reaction is believed to proceed through the catalytic cycle shown in Scheme 1.¹ Thus, the initial formation of the intermediate allenylpalladium complex **3** is followed by a series of transmetalation steps to finally generate the nucleophilic organozinc species **5**, which then adds to the carbonyl group. For propargylic mesylates **1** (X = OMs) the preferential enantio- and diastereoselective formation of anti products **2** has been conveniently rationalized by invoking chelated transition structures **6**, an interpretation which is supported by calculations performed on a simple model system.²

Our interest in the mechanism of these and related reactions arose after studies on an intramolecular variant³ revealed stereochemical tendencies that appeared to imply the intervention of “open” transition states,⁴ and similarly difficult to rationalize stereochemical outcomes were also reported on the closely related enantioselective Et₂Zn/Pd⁰-promoted allylation reaction.⁵ These and other related data,^{6–9} together with the realization that the

Scheme 1. Intermolecular Propargylation of Aldehydes with Et₂Zn/Pd⁰



mechanism of the transmetalation step, common to many Pd-catalyzed reactions, is only poorly understood in most cases,^{10,11} prompted us to undertake a computational study in order to investigate the mechanism of the Pd⁰/Et₂Zn-mediated propargylation of carbonyl compounds. We have focused our study on the **4** → **5** → **2** portion of the catalytic cycle, involving step 2 of the transmetalation process and the subsequent carbonyl addition step. As will be described below, a pathway has been found that leads to the homopropargyl alcohol product through bimetallic Pd–Zn-bonded complexes, where the Pd–Zn bond plays a key role to facilitate transmetalation. The results presented here suggest a new framework to study these and related reactions.

(10) The Stille reaction is an exception where recent experimental^{11a} as well as computational studies^{11b–d} have contributed to the rationalization of the known facts. The Suzuki reaction has also been recently the subject of detailed theoretical studies.^{11e–i}

(11) (a) Echavarren, A. M.; Cárdenas, D. J. In *Metal-Catalyzed Cross-Coupling Reactions*, 2nd ed.; de Meijere, A., Diederich, F., Eds.; Wiley-VCH: Weinheim, Germany, 2004; Vol. 1, pp 1–40. (b) Alvarez, R.; Nieto Faza, O.; Silva Lopez, C.; de Lera, A. R. *Org. Lett.* **2006**, *8*, 35–38. (c) Nova, A.; Ujaque, G.; Maseras, F.; Lledós, A.; Espinet, P. *J. Am. Chem. Soc.* **2006**, *128*, 14571–14578. (d) Ariafard, A.; Lin, Z. Y.; Fairlamb, I. J. S. *Organometallics* **2006**, *25*, 5788–5794. (e) Goossen, L. J.; Koley, D.; Hermann, H. L.; Thiel, W. *J. Am. Chem. Soc.* **2005**, *127*, 11102–11114. (f) Goossen, L. J.; Koley, D.; Hermann, H. L.; Thiel, W. *Organometallics* **2006**, *25*, 54–67. (g) Braga, A. A. C.; Morgon, N. H.; Ujaque, G.; Maseras, F. *J. Am. Chem. Soc.* **2005**, *127*, 9298–9307. (h) Braga, A. A. C.; Morgon, N. H.; Ujaque, G.; Lledós, A.; Maseras, F. *J. Organomet. Chem.* **2006**, *691*, 4459–4466. (i) Braga, A. A. C.; Ujaque, G.; Maseras, F. *Organometallics* **2006**, *25*, 3647–3658.

* To whom correspondence should be addressed. E-mail: rar@uvigo.es (R.A.); jm.aurrecoechea@ehu.es (J.M.A.).

(1) (a) Tamaru, Y.; Goto, S.; Tanaka, A.; Shimizu, M.; Kimura, M. *Angew. Chem., Int. Ed. Engl.* **1996**, *35*, 878–880. (b) Tamaru, Y. *J. Organomet. Chem.* **1999**, *576*, 215–231. (c) Marshall, J. A.; Adams, N. D. *J. Org. Chem.* **1998**, *63*, 3812–3813. (d) Marshall, J. A.; Adams, N. D. *J. Org. Chem.* **1999**, *64*, 5201–5204. (e) For a review, see: Marshall, J. A. *Chem. Rev.* **2000**, *100*, 3163–3185.

(2) Gung, B. W.; Xue, X. W.; Knatz, N.; Marshall, J. A. *Organometallics* **2003**, *22*, 3158–3163.

(3) Aurrecoechea, J. M.; Arrate, M.; López, B. *Synlett* **2001**, 872–874.

(4) Kadota, I.; Hatakeyama, D.; Seki, K.; Yamamoto, Y. *Tetrahedron Lett.* **1996**, *37*, 3059–3062.

(5) Howell, G. P.; Minnaard, A. J.; Feringa, B. L. *Org. Biomol. Chem.* **2006**, *4*, 1278–1283.

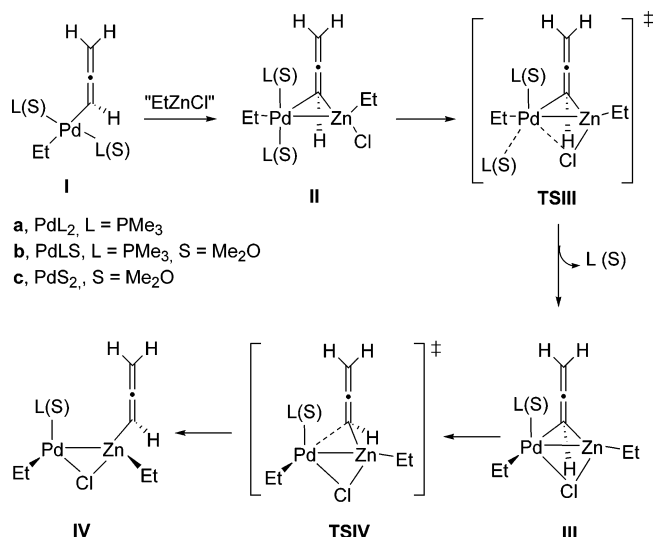
(6) Several other aspects of these reactions are not well understood. For example, the nature of the Y group on intermediate **5** remains unclear,^{1a,b,7} as does the sequence of events that leads from **3** to **5** and the remarkable absence of allene products that would arise from **4** by usually rapid reductive elimination or β -elimination events.^{1d,8} Additionally, leaving-group-dependent stereochemical outcomes have been observed in Et₂Zn/Pd⁰-promoted reactions.⁹

(7) Sakamoto, T.; Takahashi, K.; Yamazaki, T.; Kitazume, T. *J. Org. Chem.* **1999**, *64*, 9467–9474.

(8) Konno, T.; Tanikawa, M.; Ishihara, T.; Yamanaka, H. *Chem. Lett.* **2000**, 1360–1361.

(9) (a) Marshall, J. A.; McNulty, L. M.; Zou, D. *J. Org. Chem.* **1999**, *64*, 5193–5200. (b) Oppolzer, W.; Schröder, F.; Kahl, S. *Helv. Chim. Acta* **1997**, *80*, 2047–2057.

Scheme 2. Mechanism of Pd to Zn Allenyl Transfer



The starting point for calculations^{12–15} was the allenylethynylpalladium complex **I** (Scheme 2), where variants **a–c** have been used to model the two remaining ligands on palladium and to account for the fact that several types of Pd species could be involved in the catalytic cycle under the typical experimental conditions employing either Pd(PPh₃)₄^{1a,c} or, more commonly, Pd(OAc)₂/PPh₃ (1:1 ratio)^{1d} in THF. As models for PPh₃ and THF, we have used trimethylphosphine and dimethyl ether,

(12) All computations in this study have been performed using the Gaussian03 suite of programs.¹³ To include electron correlation at a reasonable computational cost, density functional theory (DFT)¹⁴ was used. The Becke three-parameter exchange functional and the nonlocal correlation functional of Lee, Yang, and Parr (B3LYP) with the 6-31G* set for C, H, Zn, O, Cl, and P, in conjunction with the Stuttgart/Dresden relativistic effective core potentials for Pd, were used to compute the geometries, energies, and normal-mode vibration frequencies of the starting material, the corresponding transition structures, and the products. We have recalculated some of the structures, namely the transformation **Iva** → **Va**, as single-point calculations with a 6-311G*/SDD basis set to further validate the results and found very minor differences (less than 0.2 kcal/mol) with a threefold more expensive cost on CPU time. The stationary points were characterized by means of harmonic analysis, and for all the transition structures, the vibration related to the imaginary frequency corresponds to the nuclear motion along the reaction coordinate under study. In selected cases where IRC calculations proved troublesome, relaxed scans along the relevant reaction coordinates were performed in order to confirm the nature of the transition states through a better understanding of the surrounding potential energy surface (PES). Solvent effects were taken into account with sequential single-point calculations at the gas-phase optimized B3LYP/6-31G* geometries using the polarized continuum model (PCM).¹⁵

(13) Frisch, M. J.; Trucks, G. W.; Schlegel, H. B.; Scuseria, G. E.; Robb, M. A.; Cheeseman, J. R.; Montgomery, J. A., Jr.; Vreven, T.; Kudin, K. N.; Burant, J. C.; Millam, J. M.; Iyengar, S. S.; Tomasi, J.; Barone, V.; Mennucci, B.; Cossi, M.; Scalmani, G.; Rega, N.; Petersson, G. A.; Nakatsuji, H.; Hada, M.; Ehara, M.; Toyota, K.; Fukuda, R.; Hasegawa, J.; Ishida, M.; Nakajima, T.; Honda, Y.; Kitao, O.; Nakai, H.; Klene, M.; Li, X.; Knox, J. E.; Hratchian, H. P.; Cross, J. B.; Bakken, V.; Adamo, C.; Jaramillo, J.; Gomperts, R.; Stratmann, R. E.; Yazyev, O.; Austin, A. J.; Cammi, R.; Pomelli, C.; Ochterski, J. W.; Ayala, P. Y.; Morokuma, K.; Voth, G. A.; Salvador, P.; Dannenberg, J. J.; Zakrzewski, V. G.; Dapprich, S.; Daniels, A. D.; Strain, M. C.; Farkas, O.; Malick, D. K.; Rabuck, A. D.; Raghavachari, K.; Foresman, J. B.; Ortiz, J. V.; Cui, Q.; Baboul, A. G.; Clifford, S.; Cioslowski, J.; Stefanov, B. B.; Liu, G.; Liashenko, A.; Piskorz, P.; Komaromi, I.; Martin, R. L.; Fox, D. J.; Keith, T.; Al-Laham, M. A.; Peng, C. Y.; Nanayakkara, A.; Challacombe, M.; Gill, P. M. W.; Johnson, B.; Chen, W.; Wong, M. W.; Gonzalez, C.; Pople, J. A. *Gaussian 03*, revision C.02; Gaussian, Inc.: Wallingford, CT, 2004.

(14) (a) Parr, R. G.; Yang, W. *Density Functional Theory of Atoms and Molecules*; Oxford University Press: New York, 1989. (b) Ziegler, T. *Chem. Rev.* **1991**, *91*, 651–667. (c) Lee, C.; Yang, W.; Parr, R. G. *Phys. Rev. B* **1988**, *37*, 785–789.

(15) (a) Onsager, L. *J. Am. Chem. Soc.* **1936**, *58*, 1486–1493. (b) Tomasi, J.; Persico, M. *Chem. Rev.* **1994**, *94*, 2027–2094. (c) Tomasi, J.; Mennucci, B.; Cammi, R. *Chem. Rev.* **2005**, *105*, 2999–3094.

respectively. As for the Zn reagent, EtZnX (X = leaving group in **1**) is usually assumed to be the transmetalating species for step 2,^{1e} and the actual choice of EtZnCl as the model is justified by literature precedents which show that propargylic halides act as effective substrates for the Et₂Zn/Pd⁰-mediated propargylation of aldehydes.^{1a} Cartesian coordinates and SCF energies of all computed structures, together with tabulated thermodynamic magnitudes and representative optimized geometries, are given as Supporting Information.

With **I** or variants with either a vacant position on Pd or a (η^3 -propargyl)palladium structure as the starting point, all attempts to find a direct transmetalation pathway through a four-centered transition state^{11a} failed, a major complication being the strong tendency of Pd and Zn to form a Pd–Zn bond,¹⁶ resulting in the formation of bimetallic complexes. Thus, the direct interaction of EtZnCl with **I** led, with no activation energy (we were unable to locate transition structures corresponding to this transformation), to the new complexes **II**, where the original Pd ligands nearly maintained their square-planar geometry while the Pd–Zn bond had an approximate perpendicular orientation with respect to that plane (see Figure 3 in the Supporting Information). Thus, a five-coordinate Pd complex results with Zn approximately occupying the apical position in a highly distorted square-pyramidal structure.¹⁷ Interestingly, Zn adopts a tetrahedral geometry in these complexes.¹⁸ Taking **Ia** as an example, the Pd–Zn distance was 2.75 Å, which is close to the corresponding distance in a 1:1 ZnPd alloy (2.65 Å).¹⁹ The most salient feature of these species is the presence of a three-membered ring²⁰ with simultaneous interactions between Zn, Pd, and the allenic carbon directly bonded to the metal, as revealed by Pd–C and Zn–C bond distances of 2.19 Å (up from 2.13 Å in **Ia**) and 2.24 Å, respectively, for **Ia**. Nonetheless, it is interesting that **Ia** has still the structural features of a somewhat distorted allenylpalladium, as indicated by C_{sp}–C_{sp}²–Pd and C_{sp}–C_{sp}²–Zn bond angles of 135.0 and 94.5°, respectively. Similarly, with **Ib** or **Ic** as the starting point, coordination of EtZnCl leads to **Iib** and **Iic**, respectively, with geometric features which are similar to those of **Ia**, except that the square-pyramidal structure is more distorted in **Iib**. Formation of **II** from **I** and EtZnCl is exothermic in all cases (Table 1). We have also computed the energetics of formation of bimetallic complexes **II** using EtZnCl-(OMe)₂ as a more realistic model for tetrahedral zinc in solution.^{18,21} As seen in Table 1, this transformation is nearly thermoneutral for **Ia** and quite favorable for **Ib** and **Ic**, which would be more appropriate models for the starting palladium species under the prevailing experimental conditions.^{1d}

Of possibly greater significance in the context of this work, in all cases a transmetalation pathway has been found that leads

(16) For an overview of alloyed Pd–Zn bimetallic catalysts, see: Coq, B.; Figueras, F. *J. Mol. Catal. A* **2001**, *173*, 117–134.

(17) DFT calculations performed on the Pd(0)-catalyzed insertion of arynes into the Sn–C σ -bond of alkynylstannanes have revealed a related five-coordinate Pd complex with a three-membered Pd–Sn–C_{sp} ring that participates in an oxidative-addition–Sn-migration step. This pathway, which appears to be a minor one in that Pd-catalyzed reaction, is however the most favorable one when Pt replaces Pd in the calculations. See: Matsubara, T. *Organometallics* **2003**, *22*, 4297–4304.

(18) The X-ray structure of EtZnCl displays tetrahedral Zn atoms coordinated to one ethyl and three chloride ligands: Guerrero, A.; Hughes, D. L.; Bochmann, M. *Organometallics* **2006**, *25*, 1525–1527.

(19) Rodriguez, J. A.; Kuhn, M. *J. Phys. Chem.* **1996**, *100*, 381–389.

(20) The interaction between Me₂Zn and Ni(0) has been similarly suggested, on the basis of DFT calculations, to lead to the formation of a bimetallic Ni–C–Zn three-membered ring with a Ni–Zn bond and a bridging methyl group: Hratchian, H. P.; Chowdhury, S. K.; Gutiérrez-García, V. M.; Amarasinghe, K. K. D.; Heeg, M. J.; Schlegel, H. B.; Montgomery, J. *Organometallics* **2004**, *23*, 4636–4646.

(21) Formation of **II** from **I** and EtZnCl(OMe)₂ appears to be a multistep process, which is presently under study.

Table 1. Overall Reaction Free Energies (kcal/mol) for Formation of Bimetallic Pd–Zn Complexes **II from **I** and EtZnCl or EtZnCl(OMe)₂ at 298 K (Gas Phase)**

entry	react ^a	ΔG
1	Ia + EtZnCl → IIa	-3.7
2	Ia + EtZnCl(S) ₂ → IIa + 2S	0.2
3	Ib + EtZnCl → IIb	-8.8
4	Ib + EtZnCl(S) ₂ → IIb + 2S	-4.9
5	Ic + EtZnCl → IIc	-11.2
6	Ic + EtZnCl(S) ₂ → IIc + 2S	-7.3

^a S = Me₂O.

from **II** to the allenylzinc species **IV** in two stages. The first step features ligand dissociation assisted by a lone pair from the neighboring Cl bound to Zn, while in the second step a fully formed allenylzinc species is generated at the expense of further weakening of the Cl–Zn bond. The ligand dissociation step generates the bicyclic allenylpalladium/zinc bimetallic structure **III**, in which a Cl occupies the position left vacant by the departing Pd ligand and additionally bridges Pd and Zn. The structures still resemble a square pyramid about the Pd center, with the zinc occupying the apical position.²² The new complexes **III** are more stable than **II** (by 3.4 kcal/mol for series **a**, 9.3 kcal/mol for series **b**, and 13.6 kcal/mol for series **c**, Figure 1). In line with the stability trends, the corresponding activation barriers are 9.3 kcal/mol for **a** but only 0.5 kcal/mol for **b** (with displacement of OMe₂),²³ while formation of **IIIc** from **IIc** is barrierless.²⁴ Significantly, the groups to be transferred upon transmetalation (allenyl and chloride) are simultaneously bound in **III** to both metals, and this is reminiscent of the cyclic four-membered arrangement customarily used as a model for transmetalation processes.^{11,25} Completion of the transmetalation process from **III** simply requires transfer of Zn–Cl to Pd–Cl bond density and breaking of the Pd–C bond, as indicated, for example, in the corresponding transition structure **TSIVa** (Figure 3 in the Supporting Information) by the lengthening of the Zn–Cl (which increases by 16% from the value in **IIIa**) and Pd–C_α bonds (47% increase) and the shortening of the Pd–Cl bond (from 2.50 Å in **IIIa** to 2.37 Å in **TSIVa**).²⁶ This step proceeds energetically uphill with activation energies of 9.2 kcal/mol for **TSIVa** and 7.4 kcal/mol for **TSIVc** in an overall endergonic process (5.9 and 3.9 kcal/mol, respectively, Figure 1). The final allenylzinc structure **IVa** maintains a cyclic three-membered PdZnCl arrangement, where net transfer of Zn–Cl to Pd–Cl bond density is indicated, for example, by Zn–Cl and Pd–Cl

(22) With **IIIa** as an example, the Zn–Cl and Pd–Cl distances are 2.43 and 2.50 Å, respectively. In comparison, X-ray diffraction data of a new dinuclear palladium complex bridged by a chlorine atom have been recently reported with Pd–Cl distances of 2.44 Å (for the Cl–PdCl–[Pd] bond) and 2.35 Å (for the ArP–Pd–Cl–[Pd] bond): Christmann, U.; Pantazis, D. A.; Benet-Buchholz, J.; McGrady, J. E.; Maseras, F.; Vilar, R. *J. Am. Chem. Soc.* **2006**, *128*, 6376–6390.

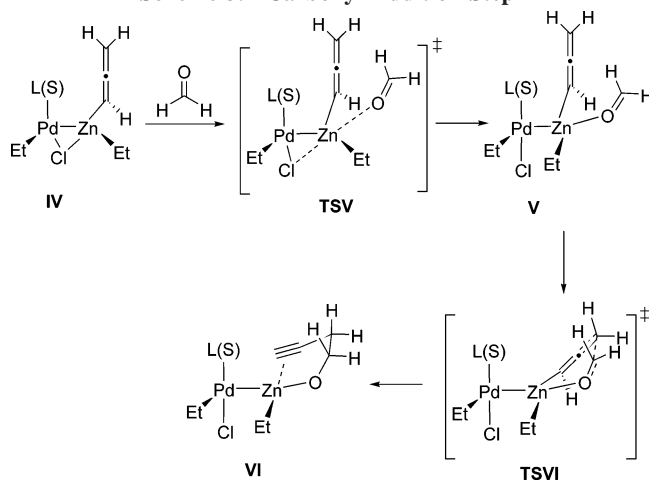
(23) The pathways starting from **Ia** and **Ib** converge at **IIIa**, implying displacement of a solvent molecule from complex **IIb**. Alternatively, a phosphine ligand could be displaced from a diastereoisomeric form of **IIb** but this pathway has a much higher activation energy (20.49 kcal/mol).

(24) The transition states **TSIIIa** and **TSIIb–IIIa** connecting **II** to **III** (confirmed with a relaxed scans calculation along the reaction coordinates) are characterized by motions associated with the imaginary frequency that reflect the weakening of the Pd–P and Zn–Cl bonds as well as the incipient formation of a Pd–Cl bond. However, we were unable to locate the corresponding transition structure for the transformation **IIc** to **IIIc**.

(25) Interestingly, a recent paper reported the X-ray crystal structure of a Ni–Al dinuclear complex with a bridging methyl group which would also be a model for a transmetalation event: Ogoshi, S.; Ueta, M.; Arai, T.; Kurosawa, H. *J. Am. Chem. Soc.* **2005**, *127*, 12810–12811.

(26) The imaginary frequency associated with the late transition state **TSIVa** (which was validated by a relaxed scans calculation along the reaction coordinates) shows the geometric changes occurring at both metal centers, Pd and Zn, in their respective conversions into the square-planar and tetrahedral geometries present in the resulting allenylzinc **IVa**.

Scheme 3. Carbonyl Addition Step



bond distances of 2.58 and 2.43 Å, respectively, in **IVa**. Therefore, in this pathway the ease of transmetalation would depend on the bridging aptitude and departing ability of halide-type and phosphine/solvent ligands, respectively, and the whole process is facilitated by the Pd–Zn bond as an element that brings the reacting fragments together.²⁷

Allenylzincs **IV** display a reactivity profile which parallels that of the simpler allenylzinc fluoride modeled by Gung and Marshall in their earlier computational study of the coupling between allenylzinc reagents and acetaldehyde.² Thus, coordination of formaldehyde to the Zn atom in **IV** takes place with displacement of a neutral Cl ligand from the coordination sphere of Zn, leading to the new complex **V** (Scheme 3). The activation energy of this step is 5.7 kcal/mol for **TSVa** and 6.6 kcal/mol for **TSVc**. The new structure **V** is already poised to undergo carbonyl propargylation through a “closed” **TSVI** (Figure 2), and this individual step requires a relatively low activation energy, regardless of the ligand used in the model (**a**, 1.8 kcal/mol; **c**, 1.5 kcal/mol). Starting from **IV**, the overall activation energies for carbonyl addition are similar in both profiles: 6.2 and 6.6 kcal/mol for **a** and **c**, respectively (Figure 1).

The geometries of transition states **TSVI**, leading to homopropargyl alkoxides **VI**, have a close resemblance with that already reported for the addition of an allenylzinc fluoride model to acetaldehyde (Figure 2).² Obvious differences arise from the presence in **TSVI** of an ethyl group and a bridging Cl in place of the reported fluoride and Me₂O ligands,² respectively, as well as, more significantly, from the incorporation of a Zn-bound Pd moiety. With **TSVIa** as an example, the Pd atom bonded to Zn maintains a distorted-square-planar structure, with an intermetallic bond distance of 2.62 Å. Significantly, the reacting carbons are placed at a distance of 2.35 Å and are oriented for nucleophilic addition (Figure 2) in an eclipsed arrangement² with a O–C_{CO}–C_{sp²}–C_{sp} dihedral angle of 26.0°.

The overall calculated gas-phase activation energies for formation of **VI** from **III** are 12.1 and 10.4 kcal/mol for the series **a** and **c**, respectively, values compatible with a reaction proceeding at temperatures in the range 0–25 °C, as reported.^{1c,d} Introduction of solvent (diethyl ether) effects in the calculations¹² lowers the energy of all the species involved (see data in the Supporting Information) but has little effect on the overall barriers (12.0 and 10.1 kcal/mol for the **a** and **c** profiles,

(27) For a synergistic effect between Pd and other metals in cross-couplings with mixed-metal catalysts, see: Shenglof, M.; Molander, G. A.; Blum, J. *Synthesis* **2006**, 111–114 and references cited therein. See also: Adams, R. D.; Captain, B.; Zhu, L. *J. Am. Chem. Soc.* **2006**, *128*, 13672–13673. Tanaka, S. I.; Hoh, H.; Akahane, Y.; Tsutsuminai, S.; Komine, N.; Hirano, M.; Komiya, S. *J. Organomet. Chem.* **2007**, *692*, 26–35.

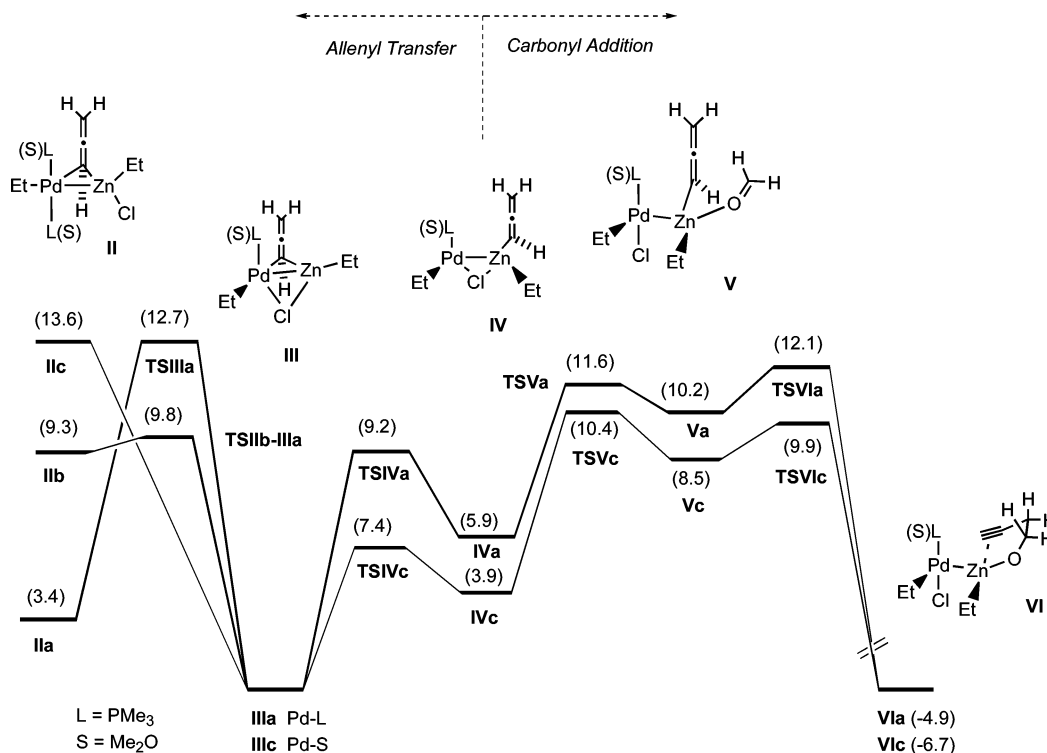


Figure 1. Energy reaction profile (gas phase) for the **I** to **VI** transformation from complexes **Ia–c**. Relative Gibbs free energies are given in kcal/mol at 298 K.

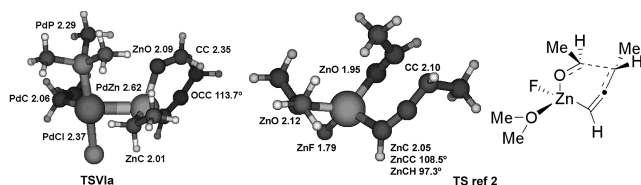


Figure 2. Transition state **TSVIa** involving C–C bond formation and comparison with the TS for carbonyl addition previously computed by Gung and Marshall.²

respectively) relative to the gas phase. On the other hand, a comparison between transmetalation/carbonyl addition pathways including either a phosphine or a solvent molecule (series **a** vs **c**) is enlightening. Thus, for the overall conversion (**II** → **VI**) our calculations predict significantly lower energy barriers (by 1.6 kcal/mol in the gas phase and by 1.9 kcal/mol in diethyl ether) when intermediate **IIIc** is involved starting from solvato complex **Ic**, as compared to pathways starting from either **Ia** or **Ib** and going through **IIIa**. Incidentally, complex **Ic** is most likely involved under the usual synthetic conditions where Pd(0) is generated from Pd(OAc)₂/PPh₃ (1:1 ratio) in a coordinating THF solvent, and this particular catalyst system has been reported to perform more effectively than Pd(PPh₃)₄ under otherwise similar conditions,^{1d} an observation that fits in well with our qualitative computational results. Furthermore, the bimetallic nature of the calculated intermediates introduces an interesting new element into the mechanistic study and may offer alternative ways to rationalize experimental facts. For example, normally facile reductive elimination and β -elimination pathways could be disfavored from Pd–Zn complexes **II** or **III** for electronic or geometric reasons, and this might explain the remarkable usual absence of the corresponding derived allene products in these propargylation reactions.^{1d,8} Additionally, both the propargylic leaving group **X** and palladium ligands are predicted to be involved all throughout the transmetalation/carbonyl addition process by means of the intermetallic link. All of these factors could modulate the acidity^{4,28} and the steric

environment of Zn and possibly be a source of unusual stereochemical results, as observed in these and related reactions.^{3,5,9}

In conclusion, DFT calculations on a portion of the catalytic cycle for the Et₂Zn/Pd⁰-mediated addition of propargylic derivatives to carbonyl compounds suggest a reaction pathway that would proceed from an allenylpalladium to a homopropargylzinc alkoxide through intermediate bimetallic Pd–Zn complexes. At this preliminary stage, the new model already accounts for some of the experimentally observed ligand effects and hints at a possible rationalization for others. A more precise mechanistic description would require characterization of the full catalytic cycle as well as the study of other variants within the same general scheme. However, it should be emphasized that the general concept highlighted here provides a new viewpoint for the mechanistic study of these reactions, which could be extended to a more general transmetalation context involving Pd/Zn as well as other metal combinations. These are ongoing studies in our laboratories.

Acknowledgment. We thank the European Commission (EPITRON, No. LSHC-CT-518417 to A.R.d.L.), the Spanish Ministerio de Ciencia y Tecnología (Grant Nos. SAF04-07131 to A.R.d.L. and CTQ2004-04901 to J.M.A., FEDER), Xunta de Galicia (Grant No. PGIDIT05PXIC31403PN to A.R.d.L.), Universidad del País Vasco (Grant No. 9/UPV00041.310-14471/2002 to J.M.A.), and Gobierno Vasco (Fellowship to A.D.) for financial support. We are indebted to the Centro de Supercomputación de Galicia (CESGA) for generous allocation of computer time.

Supporting Information Available: Tables and figures giving Cartesian coordinates and SCF energies of computed structures, tabulated thermodynamic magnitudes, and representative optimized geometries. This material is available free of charge via the Internet at <http://pubs.acs.org>.

OM061148F

(28) (a) Zweifel, G.; Hahn, G. *J. Org. Chem.* **1984**, *49*, 4565–4567. (b) Harada, T.; Katsuhira, T.; Osada, A.; Iwazaki, K.; Maejima, K.; Oku, A. *J. Am. Chem. Soc.* **1996**, *118*, 11377–11390.